Supplementary material

The following plots present:

- The vertical distribution of temperature, CO_2, CO, O, and C number densities used in the Monte Carlo simulations at 50°S, midnight local time for solar longitudes L_s = 90°, 45°, and 225° (Fig. S1).

- The evolution of the downward electron flux at 4 altitudes the electron beam penetrates the atmosphere for a 1 mW m^{-2} monoenergetic electron flux of 250 eV (Fig. S2).

- Additional results of model simulations similar to Figure 2 for the 156.1 nm carbon emission (L_s = 90°) and for the 156.1 and 165.7 nm emissions for L_s= 45° and 225° (Fig. S3 to S7).

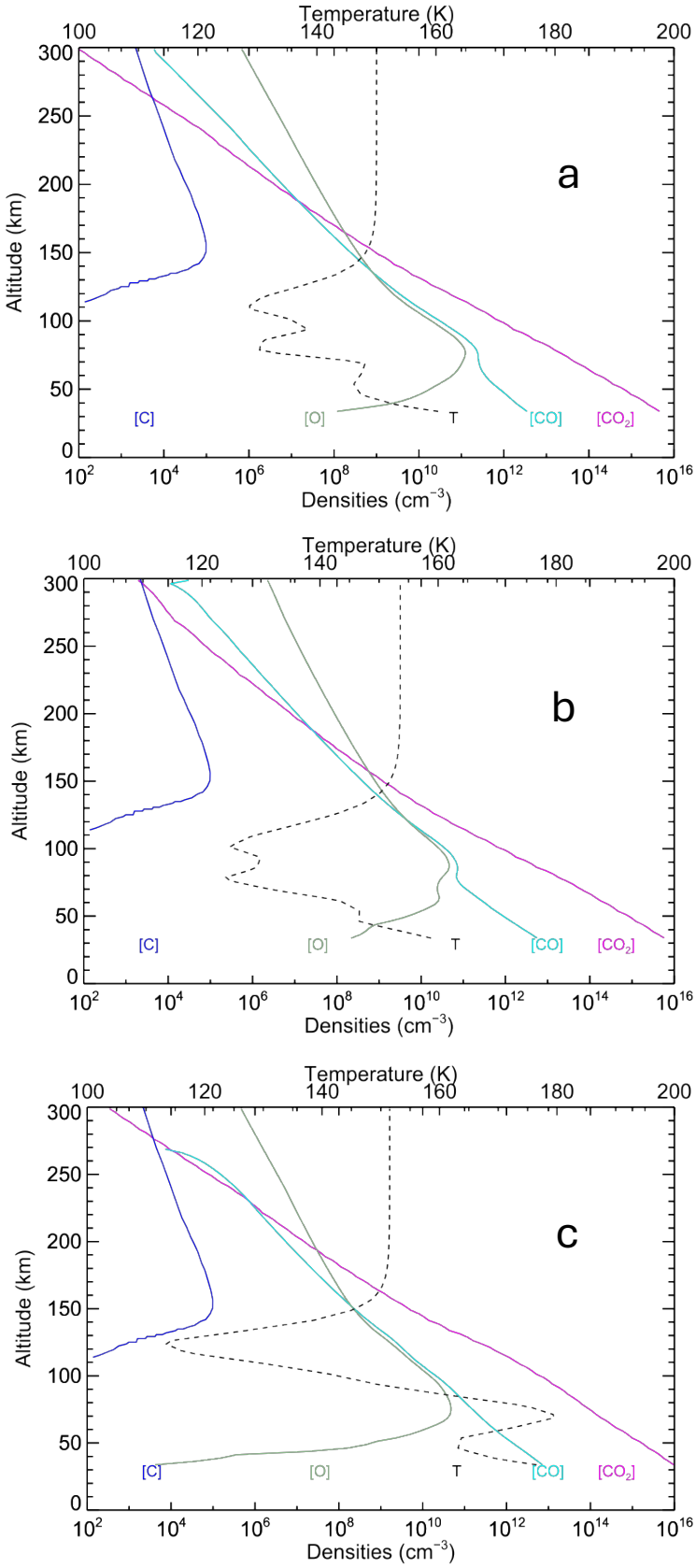

Fig. S1: vertical distribution of temperature, CO_2, CO, O, and C number densities used in the Monte Carlo simulations at 50°S, midnight local time for (a) L_s = 90°, (b) L_s = 45°, and (c) L_s = 225°.

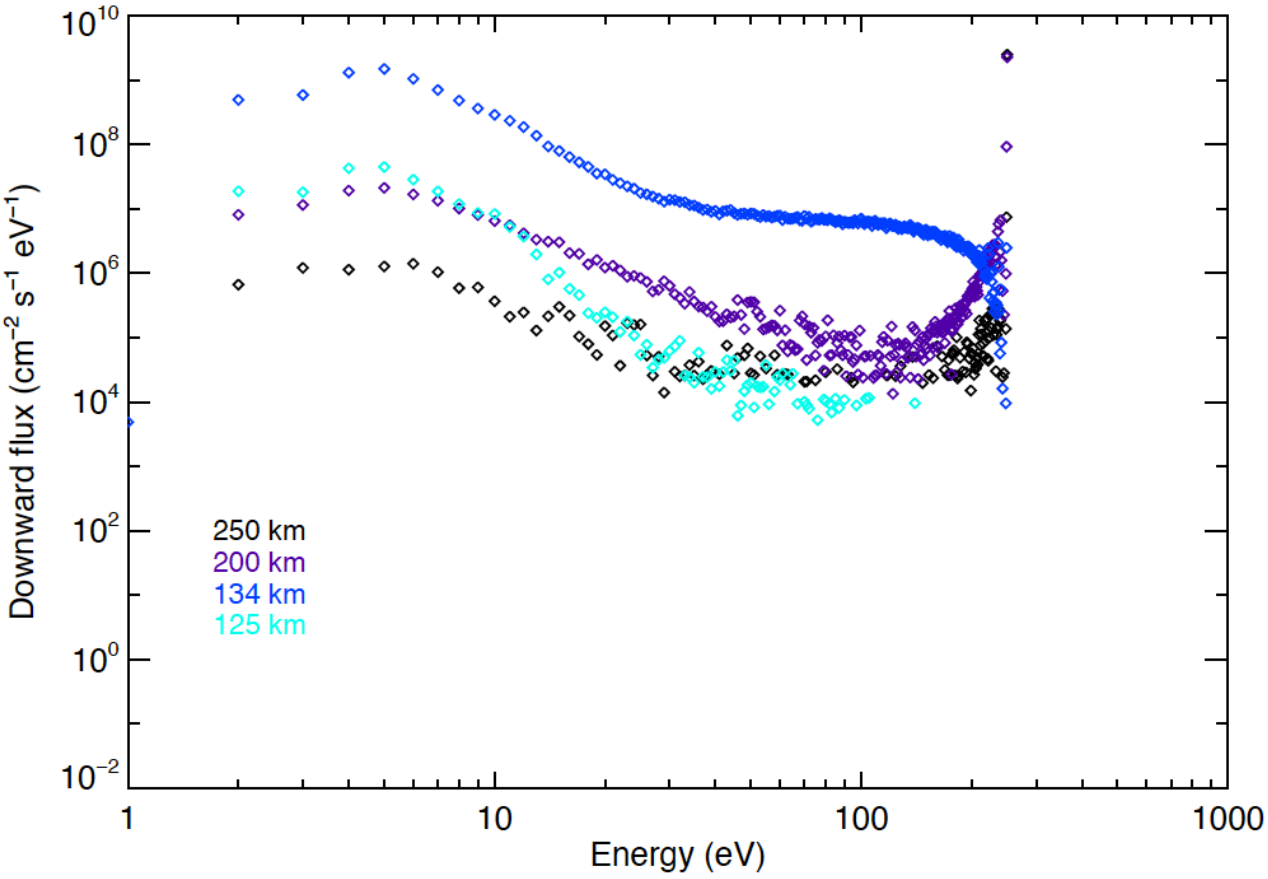

Fig. S2: calculated energy distribution of the auroral electron downward flux at 4 different altitudes for an initial monoenergetic precipitation for a 1 mW m^{-2} monoenergetic flux of 250 eV electrons. The model atmosphere is the same as described in section 2.2 and shown in figure S1a.

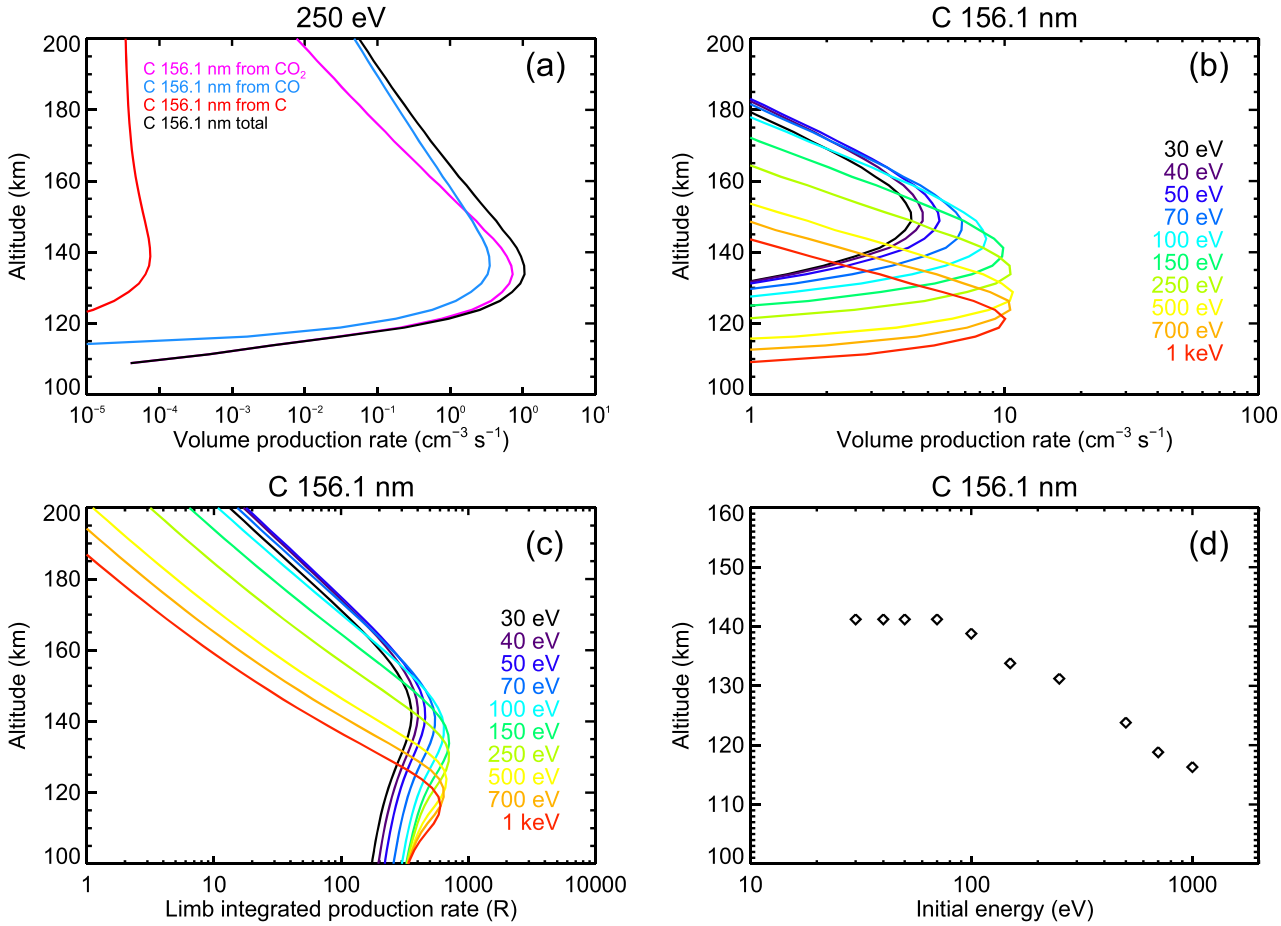

Fig. S3: (a) calculated production rates of C(^{3}D°) atoms for processes (1), (2) and (3) for an incident flux of 250 eV electrons carrying a flux of 1 mW m^{-2}, solar longitude L_s = 90°; (b) volume production rates for electron precipitation with initial energies between 30 and 1000 eV; c) limb integrated production rate corresponding to (b); (d) altitude of the maximum production as a function of the electron energy.

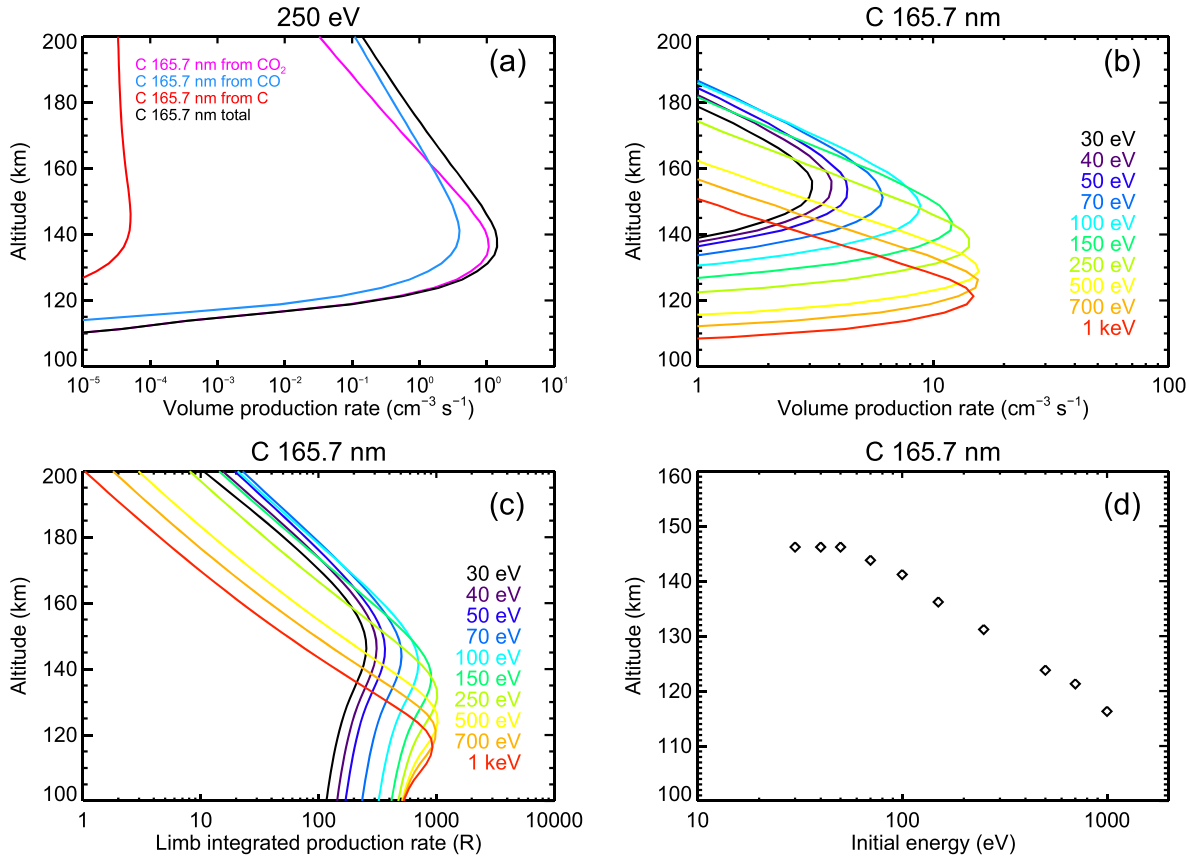

Fig. S4: (a) calculated production rates of C(^{3}P°) atoms for processes (1), (2) and (3) for an incident flux of 250 eV electrons carrying a flux of 1 mW m^{-2}, L_s = 45°; (b) volume production rates for electron precipitation with initial energies between 30 and 1000 eV; c) limb integrated production rate corresponding to (b); (d) altitude of the maximum production as a function of the electron energy.

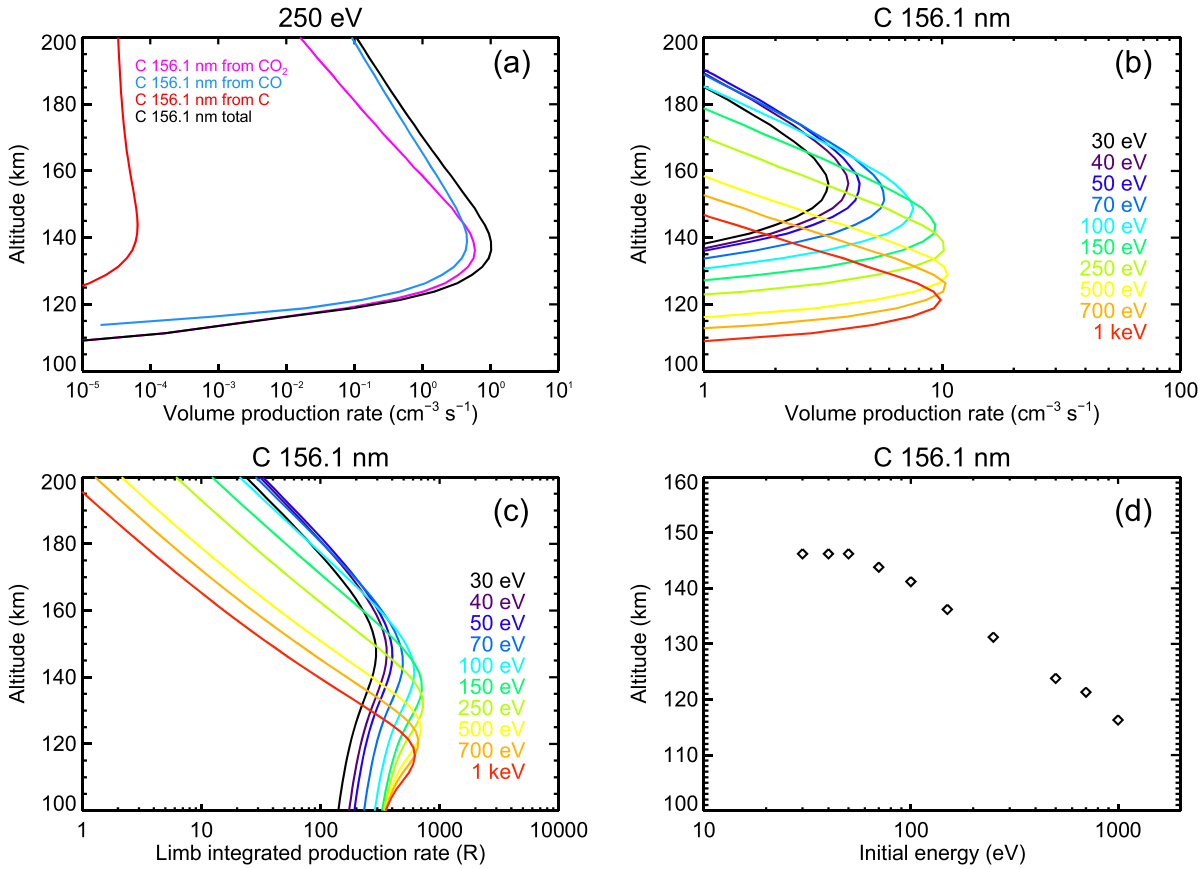

Fig. S5: (a) calculated production rates of C(^{3}D°) atoms for processes (1), (2) and (3) for an incident flux of 250 eV electrons carrying a flux of 1 mW m^{-2}, L_s = 45°; (b) volume production rates for electron precipitation with initial energies between 30 and 1000 eV; c) limb integrated production rate corresponding to (b); (d) altitude of the maximum production as a function of the electron energy.

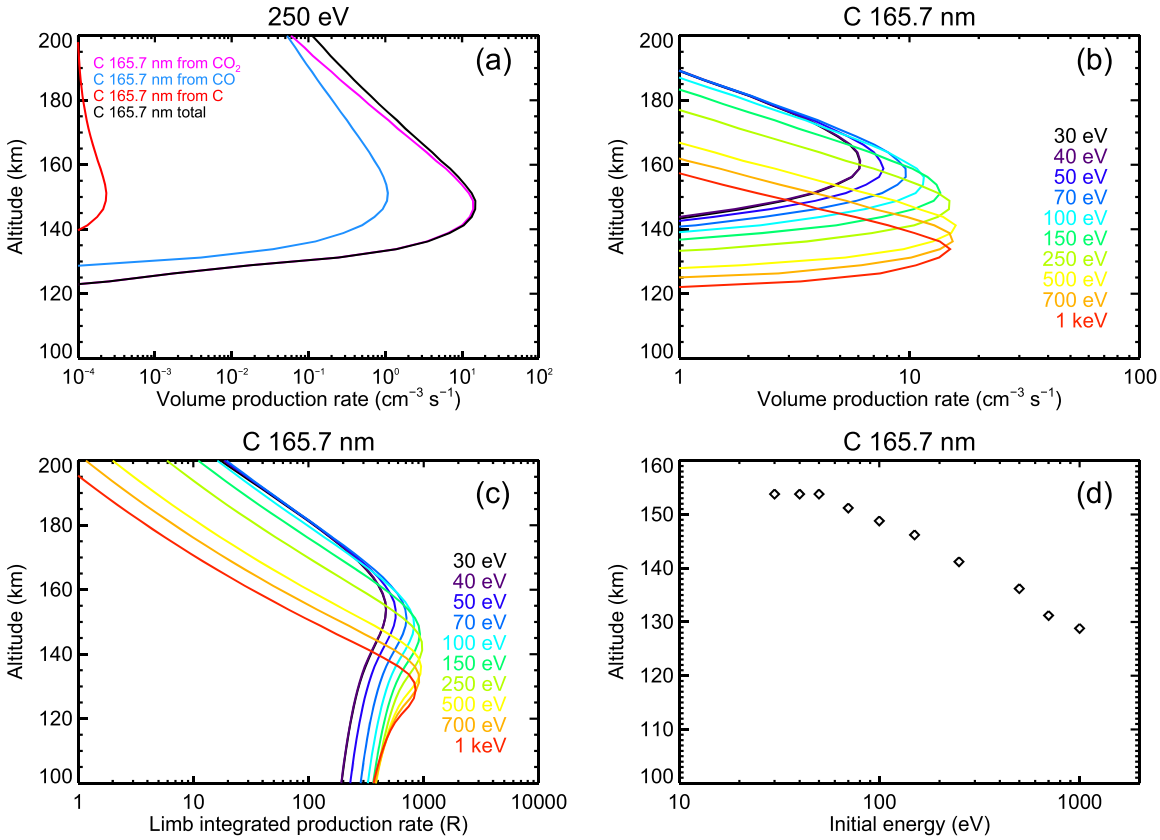

Fig. S6: (a) calculated production rates of C(^{3}P°) atoms for processes (1), (2) and (3) for an incident flux of 250 eV electrons carrying a flux of 1 mW m^{-2}, L_s = 225°; (b) volume production rates for electron precipitation with initial energies between 30 and 1000 eV; c) limb integrated production rate corresponding to (b); (d) altitude of the maximum production as a function of the electron energy.

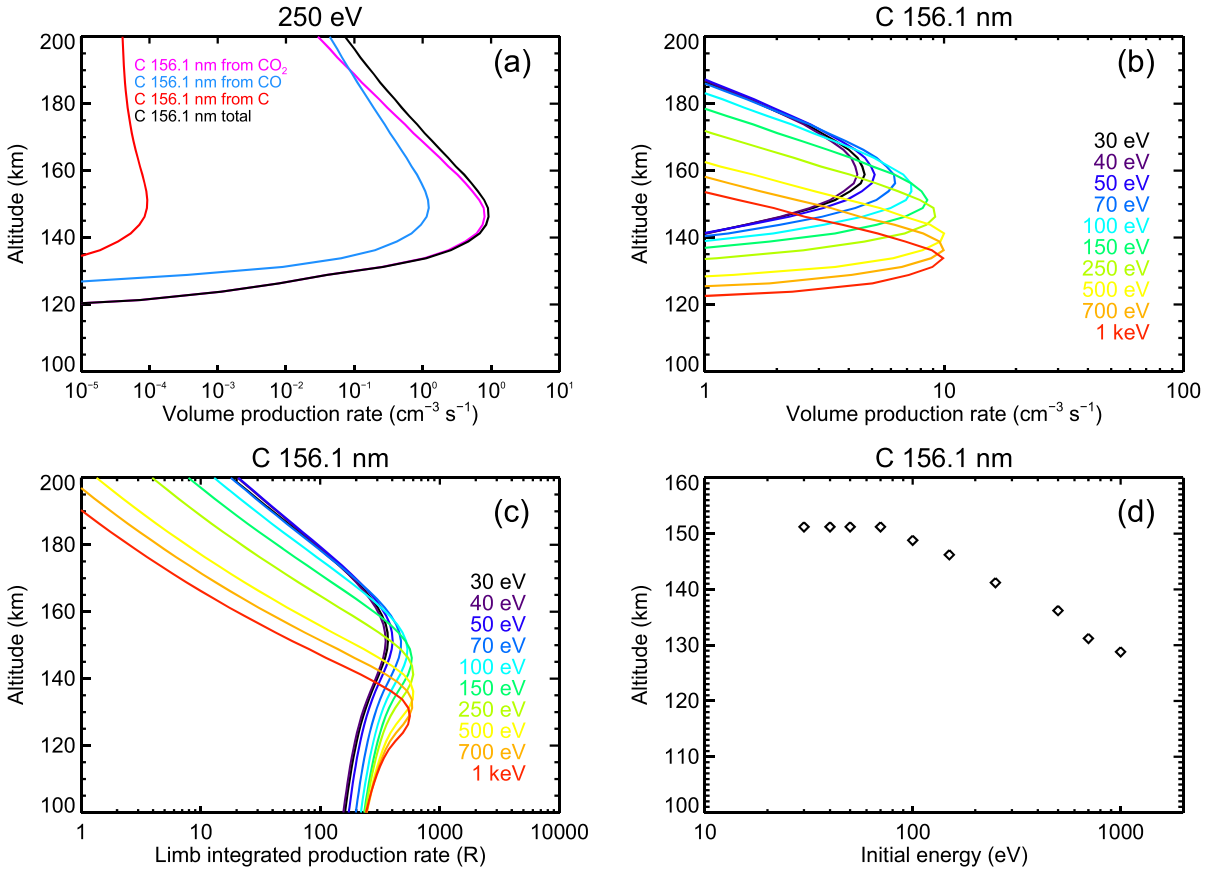

Fig. S7: calculated production rates of C(^{3}D°) atoms for processes (1), (2) and (3) for an incident flux of 250 eV electrons carrying a flux of 1 mW m^{-2}, L_s = 225°; (b) volume production rates for electron precipitation with initial energies between 30 and 1000 eV; c) limb integrated production rate corresponding to (b); (d) altitude of the maximum production as a function of the electron energy.